Optimum Temperature Policy for Sorption Enhanced Steam Methane Reforming Process for Hydrogen Production

R. Retnamma, V. Ravi Kumar, B.D. Kulkarni

This document appeared in

Detlef Stolten, Thomas Grube (Eds.):
18th World Hydrogen Energy Conference 2010 - WHEC 2010
Parallel Sessions Book 3: Hydrogen Production Technologies - Part 2
Proceedings of the WHEC, May 16.-21. 2010, Essen
Schriften des Forschungszentrums Jülich / Energy & Environment, Vol. 78-3
Institute of Energy Research - Fuel Cells (IEF-3)
Forschungszentrum Jülich GmbH, Zentralbibliothek, Verlag, 2010
ISBN: 978-3-89336-653-8

Optimum Temperature Policy for Sorption Enhanced Steam Methane Reforming Process for Hydrogen Production

Rajasree Retnamma[*], Energy Systems Modeling and Optimization Unit (UMOSE), National Laboratory of Energy and Geology (LNEG), Lisbon, Portugal
V. Ravi Kumar, **B.D. Kulkarni**, Chemical Engineering and Process Development Division, National Chemical Laboratory, Pune, India

Abstract

Sorption enhanced steam methane reforming (SE-SMR) process offers high potential for producing H_2 in fuel cell applications compared to conventional catalytic steam methane reforming (SMR) process. The reactor temperature can significantly affect the performance of the SE-SMR reaction and simultaneous adsorption behavior of CO_2. Determination of an optimal temperature policy in SE-SMR reactor is therefore an important optimization issue. Multi-stage operation is a possible way to implement optimum temperature policies. In the present work, simulation study has been carried out for multi-stage operation using a mathematical model incorporating basic mechanisms operating in a fixed bed reactor with nonlinear reaction kinetic features of an SE-SMR process. Three cases were considered for implementing the multi-stage concept and the results show that increase in temperature based on a policy leads to considerable improvement in the process performance.

1 Introduction

Sorption enhanced steam methane reforming (SE-SMR) process couples reaction and separation in a single unit and is attractive for producing H_2 in fuel cell applications. SE-SMR process uses a fixed packed column of an admixture of a SMR catalyst and an adsorbent. The adsorbent selectively removes carbon dioxide from the reaction zone and this enhances the conversion of CH_4 to H_2. The adsorbent is cyclically regenerated by using the principles of pressure swing adsorption. The reaction is highly endothermic and the determination of an optimal temperature profile is required for reducing the costs and improving the overall efficiency of operation. Coupled with multi-stage operation, it may be attractive for implementing an optimum temperature policy.

In the present work, a simulation study has been carried out on multi-stage SE-SMR process to predict optimum temperature policies for sorption enhanced steam methane reforming (SE-SMR) process. A dynamic model based on multi-component and overall mass balance, pressure distribution in the packed bed, energy balance for the bed-volume element, and non-linear Langmuir adsorption equilibrium isotherm coupled with a general reaction kinetic model was considered to predict the performance of the SE-SMR process. The linear driving force (LDF) model was used to describe the mass-transfer limited adsorption kinetics. Investigations were carried out (i) keeping inlet temperature constant for all stages (ii) step

[*] Corresponding author, email: rajasree.nair@ineti.pt

wise increase of temperature in stages to achieve maximum temperature in the last stage and (iii) increase of temperature based on a policy. The results show that increase of temperature based on a policy leads to considerable improvement in the process performance.

1.1 Mathematical model

The key chemical reactions of the SE-SMR process are given by:

$$CH_4 + H_2O \Leftrightarrow CO + 3H_2, \quad \Delta H_{298} = 206.2\ \text{kJ/mol} \tag{1}$$

$$CH_4 + 2H_2O \Leftrightarrow CO_2 + 4H_2, \quad \Delta H_{298} = 164.9\ \text{kJ/mol} \tag{2}$$

$$CO + H_2O \Leftrightarrow CO_2 + H_2, \quad \Delta H_{298} = -41.1\ \text{kJ/mol} \tag{3}$$

The mathematical model used to describe the SE-SMR process is a dynamic model and considers the non-isothermal, non-adiabatic, and non-isobaric nature of operation. The model assumptions used are:

- Axial dispersed plug flow prevails in the bed.
- Mass dispersion in the axial direction is considered.
- Mass dispersion in the radial direction is assumed to be negligible.
- The system is non-isothermal. Thermal dispersion in the axial direction is considered.
- The reaction kinetic model employed is that proposed by Xu and Froment (1989).
- Volumetric change of flow due to adsorption and reaction is taken into account in the overall material balance.
- The gas is assumed to be an ideal gas.
- The adsorbent and catalyst particles are the same size and spherical in shape.
- The pressure distribution in the packed bed adsorptive reactor is described by Ergun equation.
- The gas phase and the catalyst/adsorbent particles are assumed to be in local mass/thermal equilibrium at all times.
- The non-linear Langmuir model is used to describe the multi-component adsorption equilibrium isotherm.
- Linear driving force (LDF) model is used to represent the adsorption rate mechanism.

For the above assumptions, the reaction kinetic model, governing equations, and initial and boundary conditions are summarized below.

1. The reaction kinetic model:

   The reaction kinetic model proposed by Xu and Froment (1989) are:

$$R_I = \frac{1}{\alpha^2}\frac{k_1}{P_{H_2}^{2.5}}\left(P_{CH_4}P_{H_2O} - \frac{P_{H_2}^3 P_{CO}}{K_I}\right) \quad (4\text{ a})$$

$$R_{II} = \frac{1}{\alpha^2}\frac{k_2}{P_{H_2}^{3.5}}\left(P_{CH_4}P_{H_2O}^2 - \frac{P_{H_2}^4 P_{CO_2}}{K_{II}}\right) \quad (4\text{ b})$$

$$R_{III} = \frac{1}{\alpha^2}\frac{k_3}{P_{H_2}}\left(P_{CO}P_{H_2O} - \frac{P_{H_2} P_{CO_2}}{K_{III}}\right) \quad (4\text{ c})$$

$$\alpha = 1 + K_{CO}P_{CO} + K_{H_2}P_{H_2} + K_{CH_4}P_{CH_4} + \frac{K_{H_2O}P_{H_2O}}{P_{H_2}} \quad (4\text{ d})$$

   The formation or consumption rate r_i is then calculated by

$$r_i = \sum_{j=I}^{III} \eta_j \upsilon_{ij} R_j \quad (i = \mathrm{CH_4}, \mathrm{H_2O}, \mathrm{H_2}, \mathrm{CO_2}, \mathrm{CO}) \quad (5)$$

2. The overall mass balance equation:

$$\varepsilon_t \frac{\partial C}{\partial t} + \frac{\partial (uC)}{\partial z} + \rho_{ad} \sum_{i=1}^{n} \frac{\partial \bar{q}_i}{\partial t} - \rho_{cat} \sum_{i=1}^{n} \sum_{j=I}^{III} \upsilon_{ij} \eta_j R_j = 0 \quad (6)$$

3. The component mass balance for component i in the gas phase:

$$\varepsilon_t \frac{\partial C_i}{\partial t} + \frac{\partial (uC_i)}{\partial z} + \rho_{ad} \frac{\partial \bar{q}_i}{\partial t} - \rho_{cat} \sum_{j=I}^{III} \upsilon_{ij} \eta_j R_j = \varepsilon_b \frac{\partial}{\partial z}\left(D_L \frac{\partial C_i}{\partial z}\right) \quad (7)$$

   where, DL, the axial dispersion coefficient is evaluated by the correlation given by Edwards and Richardson (1968).

4. Pressure distribution:

   The pressure distribution in the reactor is described by Ergun equation (Ergun, 1952)

$$\frac{\partial P}{\partial z} = -K_D u - K_V u^2 \quad (8)$$

5. Adsorption Equilibrium:

   The multi-component Langmuir adsorption isotherm used to describe the adsorption equilibrium is

$$q_i^* = \frac{m_i b_i P_i}{1 + \sum_{j=1}^{n} b_i P_i} \quad (9)$$

6. Mass transfer rate:

   The Linear Driving Force (LDF) model used to describe the mass transfer of the adsorbate to the adsorbent is

$$\frac{\partial \bar{q}_i}{\partial t} = k_{fi}\left(q_i^* - \bar{q}_i\right) \tag{10}$$

   The Langmuir and LDF parameters used were as reported by Ding and Alpay (2000 a).

7. The energy balance for the bed-volume element:

$$\left[\varepsilon_t CC_{vg} + \left(\rho_{ad} + \rho_{cat}\right)C_{ps}\right]\frac{\partial T}{\partial t} + CC_{pg}u\frac{\partial T}{\partial z} - \rho_{ad}\sum_{i=1}^{n}\left(-\Delta H_{ad_i}\frac{\partial \bar{q}_i}{\partial t}\right) - \frac{2U}{R_0}\left(T_W - T\right) - \rho_{cat}\sum_{i=1}^{n}\sum_{j=I}^{III}\upsilon_{ij}\eta_j R_j \Delta H_{Rj} = \frac{\partial}{\partial z}\left(k_z\frac{\partial T}{\partial z}\right) \tag{11}$$

   where, k_z is the bed effective conductivity and is calculated using the correlation given by Yagi et al., (1960). The correlation proposed by Li and Finalyson (1977) and De Wasch and Froment (1972) is considered for calculating the wall-bed heat transfer coefficient U.

8. Initial Conditions:

   The initial conditions (at t = 0) used in the present study are as follows:

$$T = T_f,\ P_{H_2} = P_f,\ \bar{q}_i = 0$$

$$C_{H_2} = \frac{P_{H_2}}{RT_f},\ C_i = 0,\ (i = CH_4, H_2O, CO, CO_2). \tag{12}$$

   where T_f and P_f are feed gas temperature and pressure, respectively.

9. Boundary conditions:

   The following boundary conditions are used in the simulations

   (i) Reactor inlet ($z = 0$)

$$-\varepsilon_b D_L\left(\frac{\partial C_i}{\partial z}\right) = u_f\left(C_{fi} - C_i\right) \tag{13 a}$$

$$-k_z\left(\frac{\partial T}{\partial z}\right) = u_f CC_{pg}\left(T_f - T\right) \tag{13 b}$$

$$u = u_f,\ P = P_h \tag{13 c}$$

   (ii) Reactor outlet ($z = L$)

$$\frac{\partial C_i}{\partial z} = 0, \quad \frac{\partial T}{\partial z} = 0 \tag{13 d}$$

$$\frac{\partial u}{\partial z} = 0, \quad \frac{\partial p}{\partial z} = 0 \tag{13 e}$$

This is a complex system involving both reaction and separation. The reaction equilibrium constants and reaction rate constants are temperature-dependent. The adsorption

equilibrium isotherm is non-linear in nature and the equilibrium isotherm constants depend on temperature, pressure and vary with wet and dry feed conditions. Also, the above equations are coupled and cause steep composition gradient in the reactor. Equations 4-11 with appropriate initial and boundary conditions (equations 12-13) were numerically solved by finite difference method for predicting the H_2 production in the SE-SMR process. In this simulation 40 grid points along the reactor were used to obtain stable numerical solutions.

1.2 Results and discussion

Simulated results for the breakthrough curves and single stage operation were validated with experimental data given by Ding and Alpay (2000a, 2000b) for testing the accuracy of the numerical method. Three cases are considered for implementing the multi-stage concept and the results obtained are discussed below. The parameters used were as reported by Alpay (2000 b), except the column length is 0.44 m instead of 0.22 m. The maximum allowable temperature is 843 K for all three cases.

1.2.1 Case 1: Inlet temperature is kept constant at maximum feed temperature for all stages

In this case, inlet temperature of all stages is maintained at 843 K. The temperature profiles and H_2 profiles for single stage and multi-stage (2 and 3 stages) under steady state (obtained by solving the dynamic model) is plotted in figures 1-2 respectively. It is clear from figure 2 that there is not significant improvement in the process between single stage and multi-stage operation (2 and 3).

1.2.2 Case 2: Step wise increase of temperature in each stage to attain maximum feed temperature in the last stage

In this operation, maximum temperature is attained in the reactor by step wise increase of temperature in each stage, which depends on the number of stages, maximum allowable temperature and the temperature of the first stage. i.e., if there are N stages and T_{max} is the maximum allowable temperature, then temperature at the inlet of N^{th} stages is given by

$T_N = T_{N-1}+\Delta T$, where $\Delta T = (T_{max}-T_1)/N-1$ for $N > 1$.

Where, T_1 is the temperature of stage 1. The temperature profiles and H_2 profiles for single stage and multi-stage (2 - 6 stages) under steady state (obtained by solving the dynamic model) along the reactor is plotted in figures 3-4. It is evident from figure 4 that H_2 mole fraction along the reactor decreases with number stages.

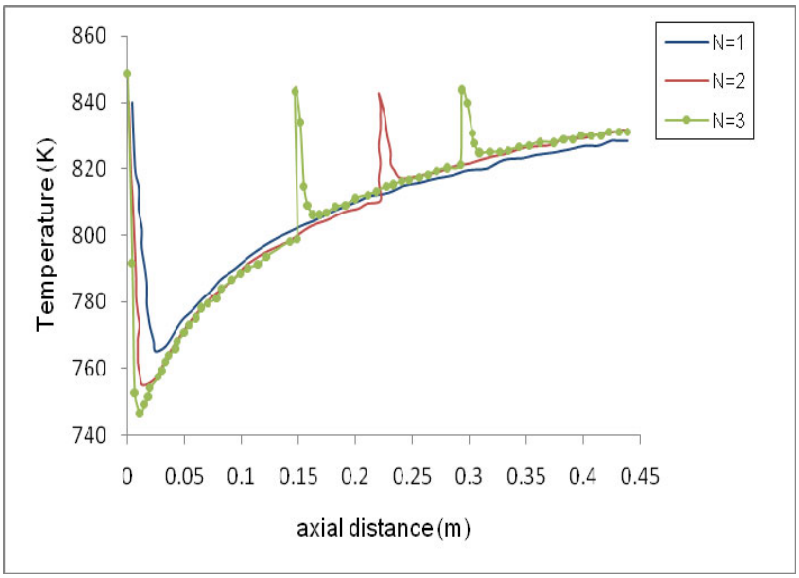

Figure 1: Temperature profiles with number of stages: Case 1.

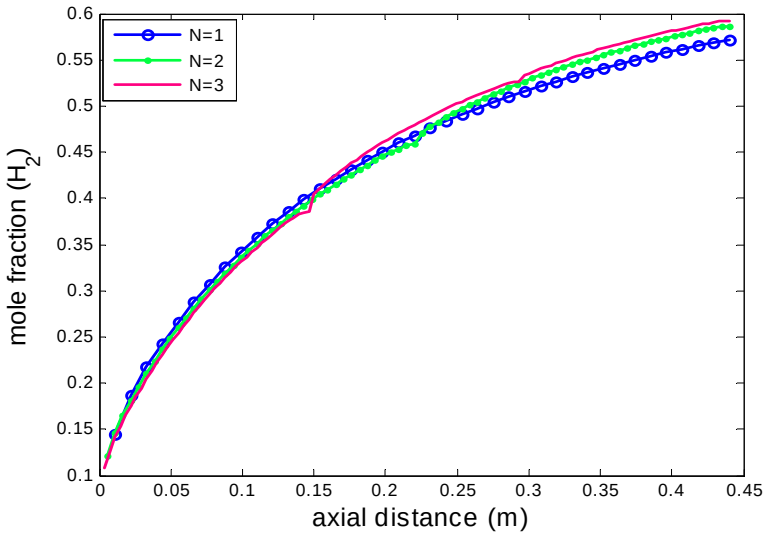

Figure 2: Concentration profiles of H_2: Case 1.

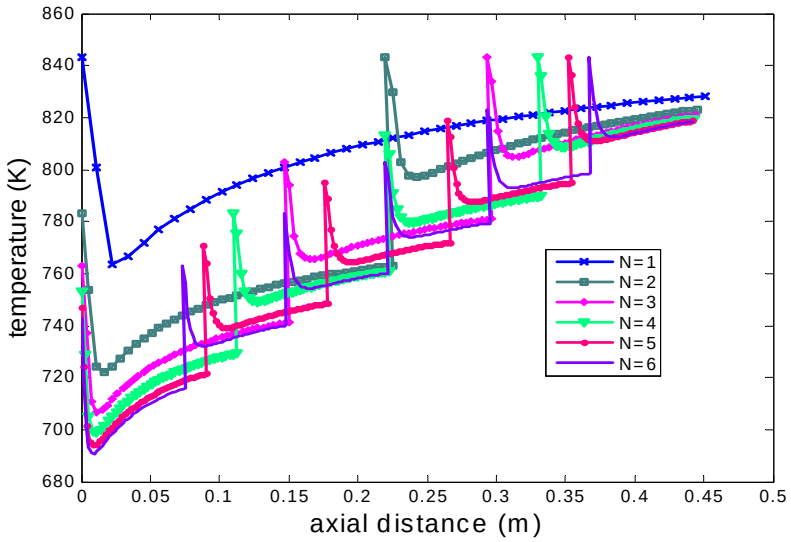

Figure 3: Temperature profiles with number of stages: Case 2.

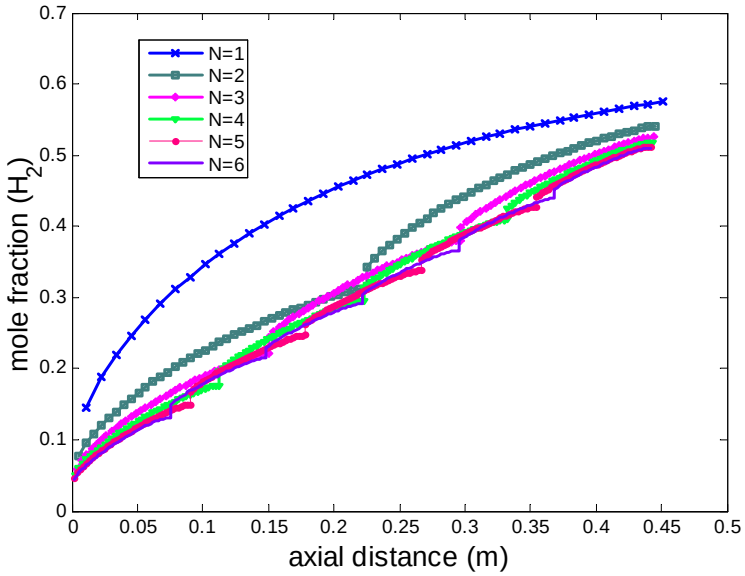

Figure 4: Concentration profiles of H_2: Case 2.

1.2.3 Case 3: Increase of temperature in each stage based on a policy

In this case, the inlet temperature of each stage is increased based on a policy with an aim to obtain an optimum temperature policy. An initial study with the temperature of the first stage is kept at 743 K and is increased by 20 K in the subsequent stages till the inlet temperature of a stage reaches 843 K was carried out to compare the results with the cases mentioned earlier. The temperature profiles and H_2 profiles for single stage and multi-stage (2 -6 stages) under steady state (obtained by solving the dynamic model) along the reactor is given in figure in figures 5-6. It is clear from figure 6 that there is a significant improvement in the process with multi-stage operation compared to a single stage.

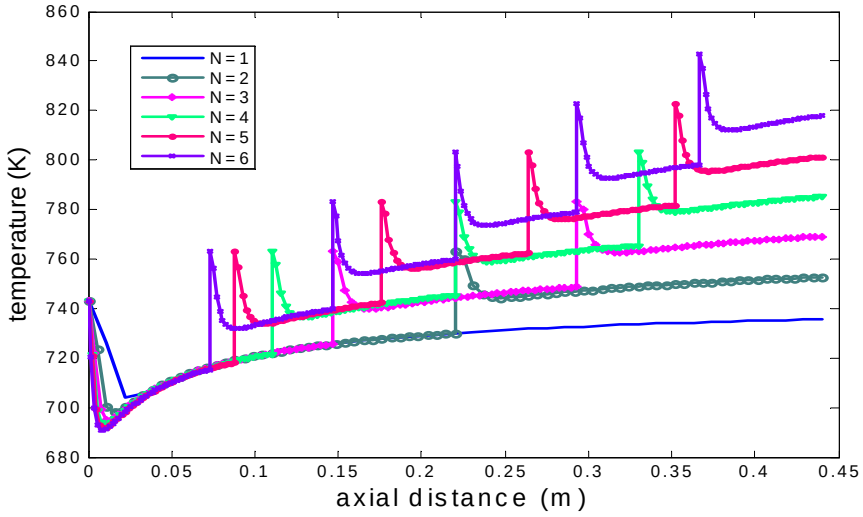

Figure 5: Temperature profiles with number of stages: Case 2.

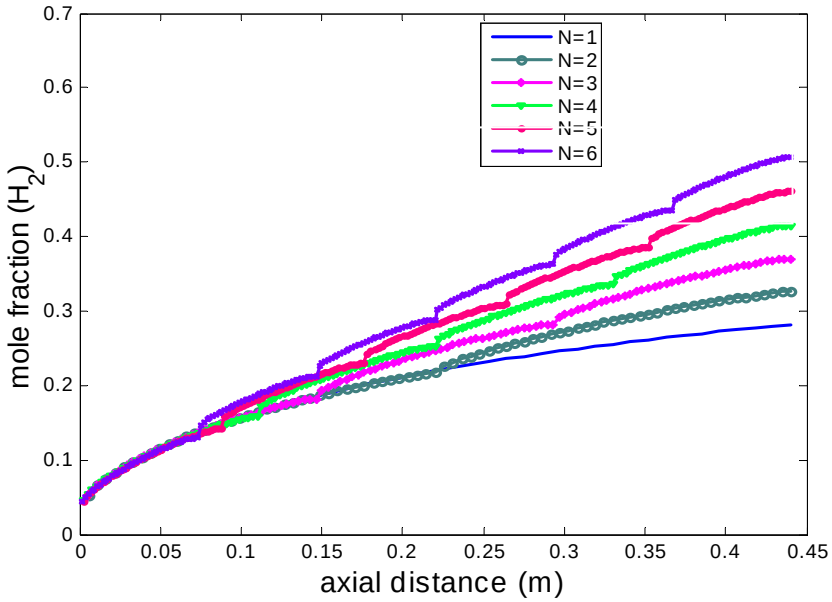

Figure 6: Concentration profiles of H_2: Case 3.

2 Conclusions

Simulation studies have been carried out for multi-stage operation of sorption enhanced steam methane reforming process for producing H_2 in fuel cell applications. Investigations on the influence of multi-stage operations led to the following conclusions: (1) there is not significant improvement in the performance of the process if the inlet temperatures of all stages are constant, (ii) step wise increase of temperature in stages to achieve maximum temperature in the last stage adversely affects the process performance, and (iii) increase of temperature based on a policy leads to considerable improvement in the process performance. The above simulation studies on multi-stage operation give insights for an

optimal temperature policy implementation in SE-SMR process for improved reactor performance.

Acknowledgement

R.R. acknowledges the Council of Scientific and Industrial Research (CSIR), New Delhi, for financial support.

Nomenclature

b_i Langmuir constant for component *i*, Pa^{-1}

c Total molar concentration in the bulk phase, mol/m^3

$c_{f\,I}$ Molar concentration of component i in the feed, mol/m^3

c_i Molar concentration of component *i*, mol/m^3

c_{pg} Gas-phase heat capacity, J/mol. K

c_{ps} Solid-phase heat capacity, J/kg. K

D_L Axial dispersion coefficient, m^2/s

$k_{f\,i}$ LDF mass-transfer coefficient of component *i*, s^{-1}

k_i Rate constant of reaction *i*, *i* = 1, 2; mol $Pa^{0.5}$/kg-cat. s, *i* = 3; mol/kg-cat. s. Pa

k_z Effective thermal conductivity, J/m.s.K

K_D Ergun equation coefficient, $N.s/m^4$

K_i Equilibrium constant of reactions (1)-(3), *i* = I, II; Pa^2, *i* = III; dimensionless

K_V Ergun equation coefficient, $N.s^2/m^5$

K_j Adsorption coefficient for component *j* (on catalyst surface), *j* = CO, H_2, CH_4; Pa, *j* = H_2O; dimensionless

k_z Effective thermal conductivity, J/m.s.K

L Reactor length, m

m_i Langmuir model constant for component *i*, mol/kg

P Local total pressure, Pa

P_h Feed pressure, Pa

P_i Partial pressure of gas-phase component *i*, Pa

$\bar{q}_i$ Solid phase concentration for component *i* (averaged over an adsorbent particle), mol/kg

q_i^* Equilibrium solid concentration, mol/kg

r_i Formation or consumption rate of component *i*, mol/kg-cat. s

R Universal gas constant, J/mol. K

R_0 Inner radius of the reactor, m

R_j Rate of reaction *j* (*j* = 1-3), mol/kg-cat.s

T time, s

T Temperature in bulk gas-phase, K

T_f Feed gas temperature, K

T_0 Initial bed temperature, K

T_w Wall temperature, K

u Superficial velocity, m/s

u_f Initial superficial velocity, m/s

U Overall bed-wall heat-transfer coefficient, J/m^2 . K

z Axial coordinate in the reactor, m

Greek letters

ε_b Bed porosity, dimensionless

ε_t Total bed porosity, dimensionless

η_i Catalyst effectiveness factor, dimensionless

ρ_{ad} Mass of adsorbent per bed volume, kg/m^3

ρ_{cat} Mass of catalyst per bed volume, kg/m^3

υ_{ij} Stoichiometric coefficient of component *i* in reaction *j*, dimensionless

$-\Delta H_{adi}$ Adsorption heat of component *i*, J/mol

ΔH_{Ri} Reaction heat of reaction *i*, J/mol

References

[1] A.P. De Wash, G.F. Froment, Chem. Engg. Sci. 27 (1972) 567.

[2] Y. Ding, E. Alpay, Chem. Engg. Sci., 55 (2000 a) 3461.

[3] Y. Ding, E. Alpay, Chem. Engg. Sci., 55, (2000 b) 3929.

[4] M.H. Edwards, J.F. Richardson, Chem. Engg. Sci. 23, (1968) 109.

[5] S. Ergun, Chem. Engg. Sci. 48 (1952) 89.

[6] C-H. Li, B.A. Finalayson, Chem. Engg. Sci. 32 (1977) 1055.

[7] J. Xu, G.F. Froment, N. Wakao, AIChE J. 35 (1989) 88.

[8] S.Yagi, D. Kunii, AIChE J., 35 (1989) 97.